Structure and dynamics of the SARS-CoV-2 envelope protein monomer

Alexander Kuzmin, Philipp Orekhov, Roman Astashkin, Valentin Gordeliy, Ivan Gushchin*

E-mail for correspondence: ivan.gushchin@phystech.edu

Supporting Information

Supplementary Tables S1-S2

Supplementary Figures S1-S5

Supplementary References

Table S1. List of the simulated systems and their properties.

№	Type	Protein	Number of lipids (by leaflet)	Number of waters	Number of ions (0.15 mM)	Time, μs	Simulation box size, nm^3
1, 2	CG	No PTM	POPC (206/221)	7706	Na+(84) Cl-(86)	2, 0.5	12×12×11 (rectangular)
3	CG	CYSP40	POPC (205/221)	7711	Na+(84) Cl-(86)	0.5	12×12×11 (rectangular)
4	CG	CYSP43	POPC (206/221)	7580	Na+(82) Cl-(84)	0.5	12×12×11 (rectangular)
5	CG	CYSP44	POPC (205/221)	7609	Na+(83) Cl-(85)	0.5	12×12×11 (rectangular)
6	CG	CYSP40/43	POPC (206/221)	7599	Na+(83) Cl-(85)	0.5	12×12×11 (rectangular)
7	CG	CYSP40/44	POPC (205/220)	7605	Na+(83) Cl-(85)	0.5	12×12×11 (rectangular)
8	CG	CYSP43/44	POPC (204/221)	7600	Na+(83) Cl-(85)	0.5	12×12×11 (rectangular)
9	CG	CYSP40/43/44	POPC (205/219)	7616	Na+(83) Cl-(85)	0.5	12×12×11 (rectangular)
10	CG	ASNG66	POPC (202/221)	12709	Na+(139) Cl-(141)	0.5	12×12×15 (rectangular)
11	CG	TMD, no PTM	POPC (222/219)	7934	Na+(88) Cl-(86)	0.5	12×12×11 (rectangular)
12	CG	H2+H3, no PTM	POPC (207/225)	7654	Na+(82) Cl-(86)	0.5	12×12×11 (rectangular)
13	AA	No PTM (1)	POPC (174/180)	31286	Na+(84) Cl-(86)	0.1×3	11×11×12 (hexagonal)
14	AA	No PTM (2)	POPC (171/179)	31304	Na+(85) Cl-(87)	0.1×3	11×11×12 (hexagonal)
15	AA	No PTM (3)	POPC (169/179)	30882	Na+(84) Cl-(86)	0.1×3	11×11×12 (hexagonal)
16	AA	No PTM (4)	POPC (174/179)	31104	Na+(84) Cl-(86)	0.1×3	11×11×12 (hexagonal)

17	AA	No PTM (1)	Mixture: POPC (100/100), POPE (50/50), POPI (20/20), POPS (10/10), CHOL (20/20)	34215	Na+(151) Cl-(93)	0.1×3	11×11×12 (hexagonal)
18	AA	No PTM (2)		32677	Na+(146) Cl-(88)	0.1×3	11×11×12 (hexagonal)
19	AA	No PTM (3)		32243	Na+(145) Cl-(87)	0.1×3	11×11×12 (hexagonal)
20	AA	No PTM (4)		35190	Na+(155) Cl-(97)	0.1×3	11×11×12 (hexagonal)
21, 22	CG	2×No PTM (X)	POPC (946/950)	64695	Na+(710) Cl-(714)	1	25×20×21 (rectangular)
23	CG	2×No PTM (XY)	POPC (759/761)	52249	Na+(573) Cl-(577)	1	21×21×20 (rectangular)
24	CG	4×No PTM	POPC (3998/3997)	105411	Na+(10493) Cl-(10501)	1	50×50×10 (rectangular)

Table S2. Properties of the TM helices in experimentally determined structures of single-helical viroporins.

Protein and virus name	Method	Membrane mimetic	TM residues (length)	Tilt angle	PDB ID	Reference
M2, Influenza A	NMR	DOPC/DOPE	26-46 (21)	32° (N-term) 22° (C-term), pH 7.5	2L0J	[1]
M2, Influenza A	NMR	DMPC	26-46 (21)	30° (N-term) 19° (C-term), pH 7.5	2KQT	[2]
M2, Influenza A	X-ray	OG	25-46 (22)	~35° (N-term), pH 7.3	3BKD	[3]
M2, Influenza A	X-ray	OG	25-46 (22)	16° (pH 7.5-8) 31° (pH 6.5) 38° (pH 3-4)	3LBW	[4]
M2, Influenza B	NMR	POPE, POPC/POPG	6-28 (23)	14° (pH 7.5) 20° (pH 4.5)	6PVR, 6PVT	[5]
Monomeric Vpu, HIV-1	NMR	DMPC	8-25 (18)	25°	2N28	[6]
Vpu, HIV-1	NMR	DOPC/DOPG	8-25 (18)	13°	1PI7, 1PI8	[7]
E, SARS-CoV	NMR	LMPG	8-35 (28)	~24°	5X29	[8]

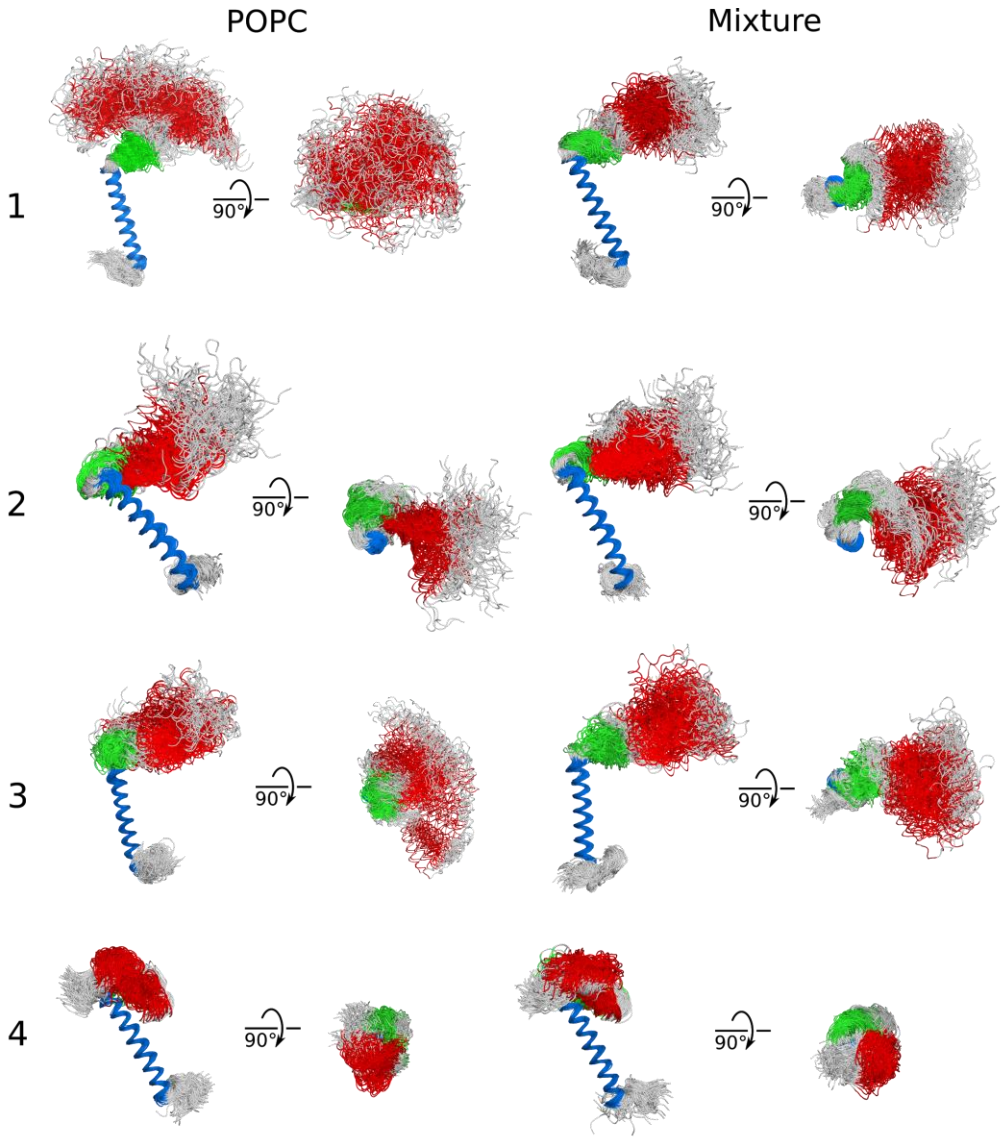

Figure S1. Conformations of the E protein observed in all-atom simulations. Positions of the transmembrane helix were aligned for clarity; helices H2 and H3 are mobile.

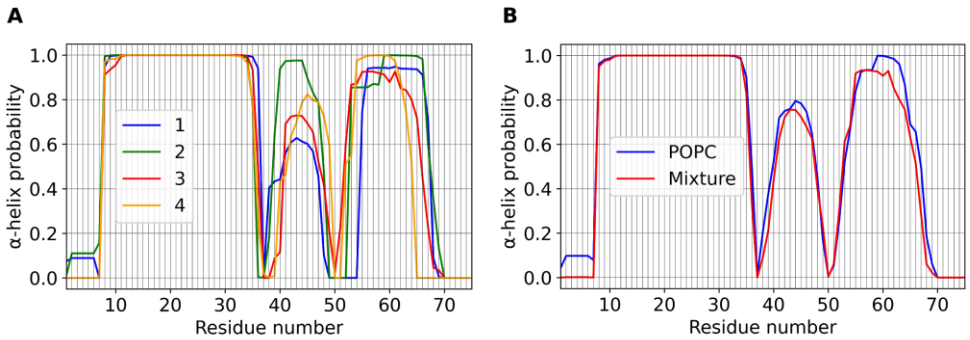

Figure S2. Conservation of the secondary structure of the E protein in AA MD simulations. Average probability of observing the α-helical structure for each residue is shown. TMD remains fully α-helical, H2 is sometimes disordered, and H3 is mostly ordered.

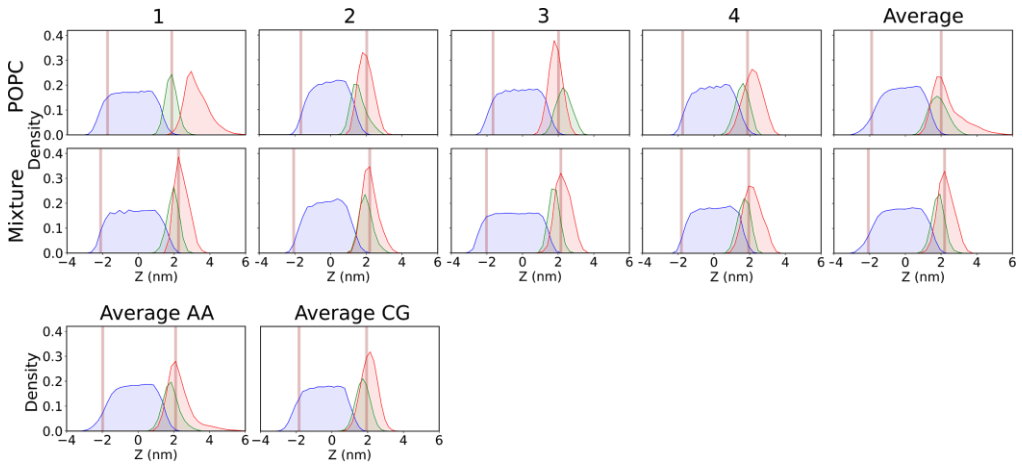

Figure S3. Average positions of TMD, H2 and H3 relative to the membrane in CG and AA simulations. Average positions of lipid phosphate groups are shown using brown lines. Distributions of TMD, H2 and H3 backbone atoms' positions are shown in blue, green and red, respectively.

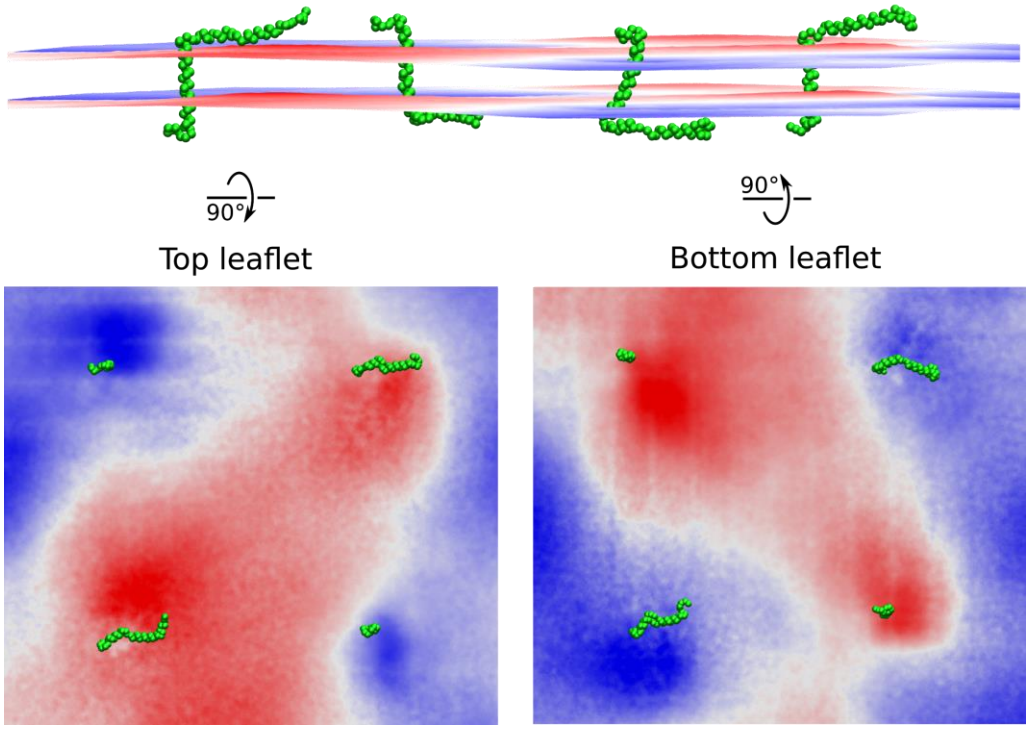

Figure S4. Induction of curvature by the E protein monomers in the system containing 4 proteins. (top) Side view of the simulated system. (left) Top monolayer. (right) Bottom monolayer. Upward displacement of each membrane boundary is shown in red, and downward displacement is shown in blue. Each panel shows an exemplary protein position; positions of the membrane boundaries are averaged over the trajectory length of 1 μs.

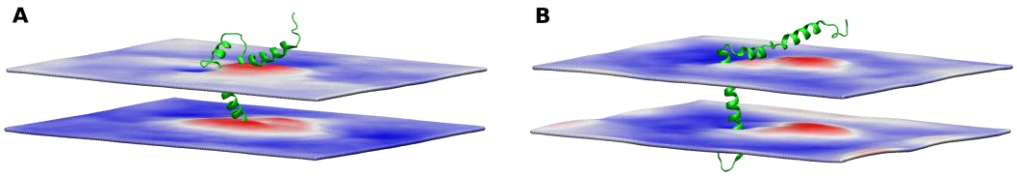

Figure S5. Induction of curvature by the E protein monomer in atomistic simulations. Upward displacement of each membrane boundary is shown in red, and downward displacement is shown in blue. (A) Induction of curvature in the POPC membrane. (B) Induction of curvature in the native-like membrane. The membrane is bent towards the α-helices H2 and H3. Each panel shows an exemplary protein position; positions of the membrane boundaries are averaged over the trajectory length.

SUPPLEMENTARY REFERENCES

[1] M. Sharma, M. Yi, H. Dong, H. Qin, E. Peterson, D.D. Busath, H.-X. Zhou, T.A. Cross, Insight into the Mechanism of the Influenza A Proton Channel from a Structure in a Lipid Bilayer, Science. 330 (2010) 509–512. https://doi.org/10.1126/science.1191750.

[2] S.D. Cady, K. Schmidt-Rohr, J. Wang, C.S. Soto, W.F. DeGrado, M. Hong, Structure of the amantadine binding site of influenza M2 proton channels in lipid bilayers, Nature. 463 (2010) 689–692. https://doi.org/10.1038/nature08722.

[3] A.L. Stouffer, R. Acharya, D. Salom, A.S. Levine, L. Di Costanzo, C.S. Soto, V. Tereshko, V. Nanda, S. Stayrook, W.F. DeGrado, Structural basis for the function and inhibition of an influenza virus proton channel, Nature. 451 (2008) 596–599. https://doi.org/10.1038/nature06528.

[4] R. Acharya, V. Carnevale, G. Fiorin, B.G. Levine, A.L. Polishchuk, V. Balannik, I. Samish, R.A. Lamb, L.H. Pinto, W.F. DeGrado, M.L. Klein, Structure and mechanism of proton transport through the transmembrane tetrameric M2 protein bundle of the influenza A virus, PNAS. 107 (2010) 15075–15080. https://doi.org/10.1073/pnas.1007071107.

[5] V.S. Mandala, A.R. Loftis, A.A. Shcherbakov, B.L. Pentelute, M. Hong, Atomic structures of closed and open influenza B M2 proton channel reveal the conduction mechanism, Nature Structural & Molecular Biology. 27 (2020) 160–167. https://doi.org/10.1038/s41594-019-0371-2.

[6] H. Zhang, E.C. Lin, B.B. Das, Y. Tian, S.J. Opella, Structural determination of virus protein U from HIV-1 by NMR in membrane environments, Biochimica et Biophysica Acta (BBA) - Biomembranes. 1848 (2015) 3007–3018. https://doi.org/10.1016/j.bbamem.2015.09.008.

[7] S.H. Park, A.A. Mrse, A.A. Nevzorov, M.F. Mesleh, M. Oblatt-Montal, M. Montal, S.J. Opella, Three-dimensional Structure of the Channel-forming Trans-membrane Domain of Virus Protein “u” (Vpu) from HIV-1, Journal of Molecular Biology. 333 (2003) 409–424. https://doi.org/10.1016/j.jmb.2003.08.048.

[8] W. Surya, Y. Li, J. Torres, Structural model of the SARS coronavirus E channel in LMPG micelles, Biochimica et Biophysica Acta (BBA) - Biomembranes. 1860 (2018) 1309–1317. https://doi.org/10.1016/j.bbamem.2018.02.017.